ELSEVIER

www.elsevier.nl/locate/carres

Carbohydrate Research 326 (2000) 194–209

CARBOHYDRATE RESEARCH

Computational studies on carbohydrates: in vacuo studies using a revised AMBER force field, AMB99C, designed for α-(1→4) linkages☆,☆☆

Frank. A. Momany *, J.L. Willett

Plant Polymer Research, USDA, ARS, National Center for Agricultural Utilization Research, 1815 N. University Street, Peoria, IL 61604, USA

Received 15 September 1999; accepted 3 January 2000

Abstract

Modifications to the AMBER force field [W.D. Cornell, P. Cieplak, C.I. Bayly, I.R. Gould, K. Merz, D.M. Ferguson, D.C. Spellmeyer, T. Fox, J.W. Caldwell, P.A. Kollman, *J. Am. Chem. Soc.*, 117 (1995) 5179–5197] have been made to improve our ability to reproduce observed molecular properties of α-linked carbohydrates when calculated using empirical potential-energy functions. Molecular structures and energies obtained using gradient-optimized density functional methods with ab initio basis sets (B3LYP/6-31G*) on ten minimum-energy conformations of maltose [F.A. Momany, J.L. Willett, *J. Comp. Chem.*, submitted for publication] were used to refine the empirical potentials. Molecular dynamics simulations on β-maltose (i.e., the β anomer of maltose), cyclohexamylose (α-cyclodextrin), cycloheptamylose (β-cyclodextrin) and larger cyclomaltooligosaccharide structures were carried out and compared with experimental structural studies to test the new potentials. Ring-puckering potential during dynamics as well as conformational transitions to 'flipped' structures were examined. Results of the tests described here suggest that the revised AMBER parameters (AMB99C) are very good for computational studies of α-(1→4)-linked carbohydrates. Published by Elsevier Science Ltd.

Keywords: Maltose; Cyclomaltooligosaccharides; Cyclodextrins; Conformation; AMB99C; Force field; Molecular mechanics; Dynamics

1. Introduction

It is common in the computational study of carbohydrates to use structural data obtained from crystallographic or NMR analysis as guides to the quality of theoretical computations. However, X-ray crystallographic data are limited to solid-state motions, and no information is readily obtained that relates to conformational transitions occurring in the solvated state of the molecule. Further, one cannot simply assume that the X-ray crystal structure will be the same as if the molecule were observed in the gas or vacuum phase, although density functional theory (DFT)/ab initio results [2] suggest strong similarities. NMR studies of carbohydrate polymers generally give very limited data on conformation

☆ Part II in the series, 'Computational Studies on Carbohydrates.' For Part I, see Ref. [2].

☆☆ Names are necessary to report factually on available data; however, the USDA neither guarantees nor warrants the standard of the product, and the use of the name by the USDA implies no approval of the product to the exclusion of others that may also be suitable.

* Corresponding author. Tel.: +1-309-6816362; fax: +1-309-6816362.

E-mail address: momanyfa@mail.ncaur.usda.gov (F.A. Momany)

0008-6215/00/$ - see front matter Published by Elsevier Science Ltd.
PII: S0008-6215(00)00042-2

because of the similarity of every sugar residue to every other sugar residue in the molecule. Therefore, to understand fully the solution dynamics and structure of a complex carbohydrate on the molecular level requires a computational method, such as molecular mechanics, to probe the energy states and dynamic motions in the environment of interest. From such computations one can attempt to explain the complicated atomic interactions that determine the conformational transitions ongoing in solution. The past decade has seen major advances in molecular mechanics techniques, particularly in molecular dynamics simulations using periodic boundary conditions, Monte Carlo searching methods and distance cutoffs and switching functions to reduce the computational times, to name a few. Further, modern empirical molecular force fields have the potential to reproduce correctly most observable structural parameters in carbohydrates, if correctly parameterized.

In this paper we describe the modifications made to the AMBER empirical force field [1] using detailed structural information derived from the authors' DFT/ab initio [2] calculations (B3LYP/6-31G*) on model carbohydrates and ab initio studies and experimental observations of other workers. Revisions in the force field parameters around the anomeric carbon of the disaccharide maltose were found to be necessary to fit the geometries and energies obtained from the DFT/ab initio calculations and simultaneously fit the experimental data described herein. This paper is not the first in which ab initio and DFT calculations have been applied to carbohydrate-like problems. Papers using molecular orbital (MO) methods have preceded this work [3–16], and the development of empirical potentials that reproduce many aspects of carbohydrate conformational transitions have been presented by other workers [17–27].

Several of the available empirical force fields (AMBER, CVFF, CFF91) were tested against our DFT/ab initio results [2] and other ab initio results and found to be inadequate for carbohydrate study. By this we mean that they were considered inadequate if the bridging dihedral angles at the minimum-energy conformation, or the energy differences between conformations, or the geometry around the anomeric carbon, were considerably removed from the equivalent values found from our DFT/ab initio results on maltose. The purpose of this paper is to describe our revisions made to the AMBER force field [1] and to tabulate structural and energetic results using the new AMB99C force field described herein. In the following paper (denoted Paper III in this series [28]), we describe solvation results using the TIP3P water potentials. Results on carbohydrates using other force fields will be presented where comparisons can be made. The force field parameters for AMB99C are listed in Appendix A.

2. Methods

Nomenclature and software.—We use the recommendations and symbols of nomenclature as proposed by IUPAC [29] throughout. The relative orientation of a pair of contiguous glucose residues is described by two torsional angles at the glycosidic linkage, denoted ϕ and ψ. For a $(1\rightarrow4)$ linkage these become (Eqs. (1) and (2)):

$$\phi = \text{O-5–C-1–O-1–C-4}' \text{ or}$$

$$\phi_{\text{H}} = \text{H-1–C-1–O-1–C-4}' \quad (1)$$

$$\psi = \text{C-1–O-1–C-4}'\text{–C-5}' \text{ or}$$

$$\psi_{\text{H}} = \text{C-1–O-1–C-4}'\text{–H-4}' \quad (2)$$

The orientation of the primary hydroxyl groups (ω) is referred to as either *gauche–trans* (*gt*), *gauche–gauche* (*gg*) or *trans–gauche* (*tg*). Using this terminology, one first states the torsion angle defined as ω (O(5)–C(5)–C(6)–O(6)), followed by C(4)–C(5)–C(6)–O(6). The hydroxylic hydrogen atoms are described by $\chi(i) =$ H–O(i)–C(i)–H(i).

A general phenomenon of interest in carbohydrate modeling is that denoted as the 'anomeric effect.' Although several explanations for the anomeric effect have been proposed, a widely held model is based on a back donation of electronic density from the lone pairs of the ring oxygen atom into an antibonding α* C-1–O-1 orbital. This analysis is supported by structural evidence such as

configuration-dependent variations in the C-1–O-1 bond lengths. We have examined the geometric and energetic consequences of the anomeric effect carefully in the development of the new AMB99C force field.

Several software programs are used to generate the carbohydrate three-dimensional structures. The MSI Biopolymers and Polymerizer 4.0 programs (Molecular Simulations, San Diego, CA) are used to generate linkages and configurations (L and D as well as α and β anomers) and conformations (ϕ, ψ) of the sequences generated. A database of monosaccharide structures is available and different linkages may be applied during the building process. Using the MSI Amorphous-Cell program, the radius of gyration may be calculated for comparison to experimental results. DFT/ab initio calculations were carried out using the Parallel Quantum Solutions version 2 software programs on the QS4–400S four parallel processor hardware (Parallel Quantum Solutions, Fayetteville, AR, 1998).

Atom typing and placing of atomic charges is carried out using the typing and charging algorithms in the MSI InsightII/4.0 software. The rules for atom typing are the same as those used for the Homans [19] modified AMBER atom types, and the charges are applied to each atom through bond group charges as found in Appendix A. The parameter file for the molecular mechanics force constants is part of the suite of files used by MSI's 4.0 Discover program and changes to these parameters are made to optimize the fit of the empirical structural parameters to the DFT/ab initio structures.

Molecular mechanics calculations.—All calculations were carried out using the modified AMBER [1,19] force field, modified as described herein and denoted AMB99C. The new force field was implemented in the MSI InsightII 4.0 Discover programs. The dielectric constant was treated as $\varepsilon = 1$ with the electrostatic and nonbonded van der Waals 1–4 terms scaled by 0.5. The scaling differs from that used in a later version of AMBER by Cornell et al. [1], who used 0.833 for electrostatic 1–4 terms and 0.5 for 1–4 nonbonded van der Waals interactions. Empirical energy minimizations were carried out to a gradient of less than ~ 0.001 kcal/mol using different minimization techniques and depending upon the size of the particular molecule or solvated system of interest. Molecular dynamics simulations were performed using the MSI 4.0 Discover program. Integration is numerically carried out using the Verlet algorithm and trajectories initiated by assigning velocity components randomly selected from a thermal distribution at 300 K to the atoms. Calculations were carried out at 300 K and time steps of 1 fs. The equilibration time was approximately 1/10 of the total simulation times, which varied from 100 ps to 1 ns in length. Explicit hydrogen atoms are included in all calculations and hydrogen atoms are allowed to move on all molecules.

The large number of possible disaccharide conformations differing only in the exocyclic C–O bonds will not be discussed in detail at this time because it has been addressed elsewhere [30]. Static energy-minimized conformations are obtained using a combination of dynamics simulations at elevated temperatures and chemical preferences for allowed conformational space. Each minimum-energy bridge (ϕ, ψ) conformation of a disaccharide is associated with a manifold of minimum-energy conformations corresponding to different values of the exocyclic torsional angles. In the case of the $-CH_2OH$ groups we adopt the preferred *gg* and *gt* conformers in vacuo and let the dynamic forces make the final decision as to the preferred position. It is found in general that the hydroxymethyl group can rotate with the AMB99C force field, and it readily takes up preferred conformations, as do all the hydroxyl groups throughout the simulations studied here. There may exist a residual conformational directing effect that is dependent upon the starting conformations, but this effect disappears after dynamic equilibration is achieved. It takes some time for the fully clockwise conformer to come to the counterclockwise conformation, but this transition occurs with this force field during dynamics. In a brief study of glucose, we followed published work [13,15].

Adiabatic ϕ, ψ isopotential contour maps for a number of disaccharides may be found in the literature and isopotential maps will not

be reproduced here, although with the revised potentials these maps have changed the shape of the isopotential energy low-energy regions (as shown by energy contours) and subsequently, the slope or change in energy as one moves toward a position of minimum energy, is changed from that found using other potentials. Rather, we will show results of a dynamics simulation where ϕ, ψ, ω and ω' position are plotted over the time of the simulation. These dynamically occupied (ϕ, ψ) regions map out the allowed regions of energy–space (at 300 K) in a much more realistic way than do static minimum energy (0 K) contour maps. Time versus (values of ω and ω') plots clearly map out side-chain conformational transitions.

Force field refinement.—Homans [19] reported on the development and testing of a modification of the AMBER force field designed to treat carbohydrates. The atom types, charges and potentials of the Homans [19] modified AMBER were used here as a starting point to test against our experimental and theoretical data. Two sets of atom types, BC, BH, OB and AC, AH, OA, are used to define the β- and α-anomeric centers, respectively (see Fig. 1). The use of two sets of atom types to describe the glycosidic bond is not a method one would prefer because it becomes impossible to compare the α with the β anomer energies. Unfortunately, the use of more complex functions (such as are used in the CFF91 and CFF95 force fields) to handle the rather large geometric anomeric effects appears not to have been fully worked out, although an attempt to parameterize a QMFF (quantum mechanics derived force field) for carbohydrates has recently been published [16]. With the restrictions imposed by having two sets of parameters at the anomeric site, it will be shown that we are able to reproduce the DFT/ab initio derived geometries very closely, while the energy differences between conformers are reasonably well fit.

We have used parameterization methods similar to those published previously [31–33], fitting geometry terms to the DFT/ab initio geometries and nonbonded terms to adjust the hydrogen-bonding distances and conformational energy differences. The fit to these last terms required changes in both partial atomic

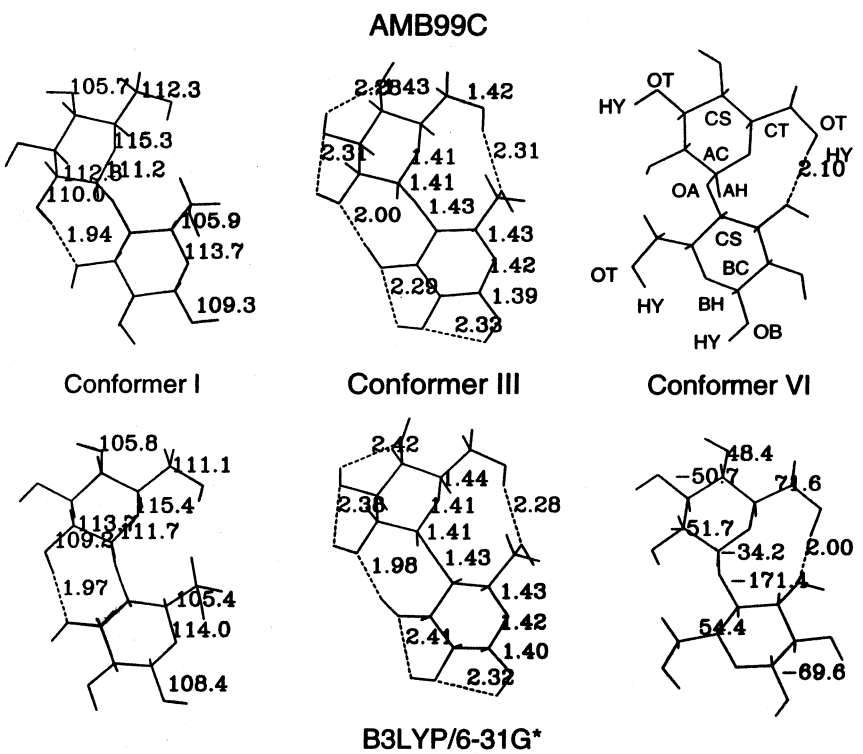

Fig. 1. Molecular parameters and atom types on Conformers I, III, and VI of Ref. [2] for B3LYP/6-31G* structures and the equivalent empirically derived AMB99C structures.

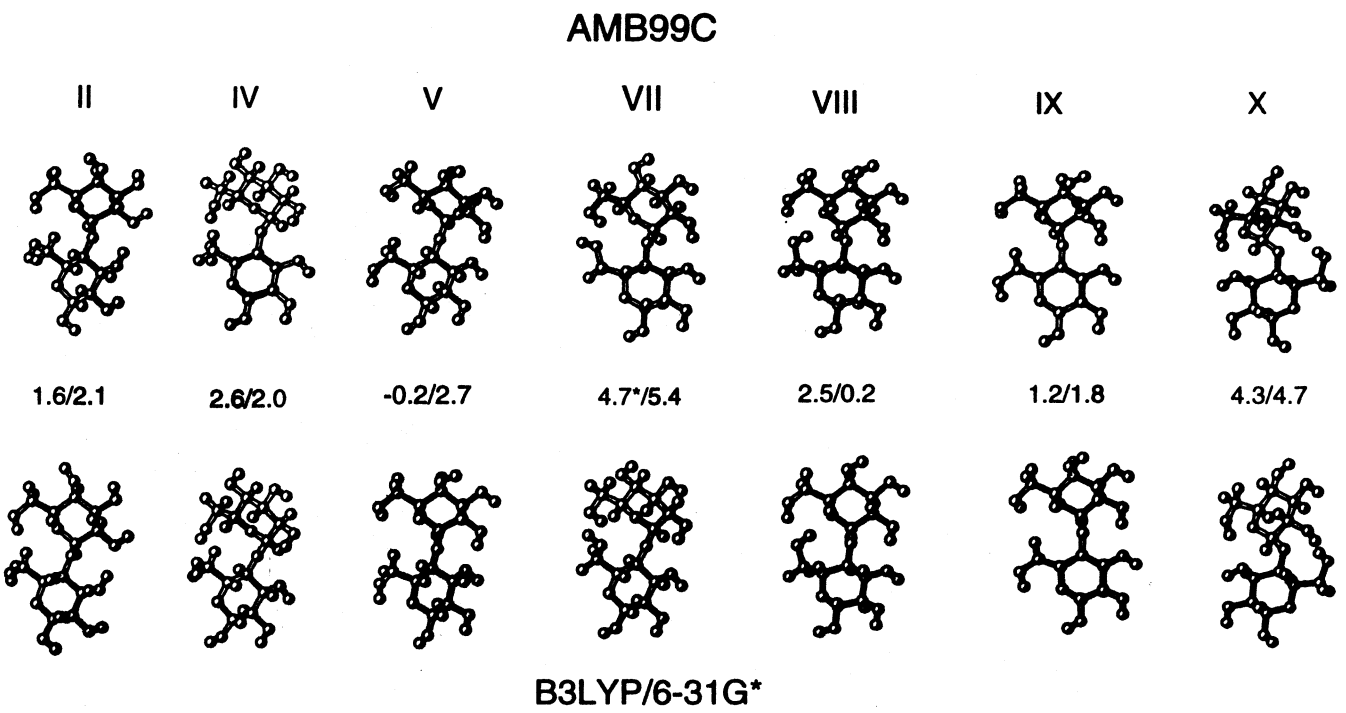

Fig. 2. Ball and stick figures of Conformers II, IV, V and VII–X. Relative energy is given for the AMB99C over B3LYP/6-31G*. In conformer VII, the * denotes that the χ^2 value moves to another conformation upon minimization. The energy given is for a conformation the same as found from the DFT/ab initio result.

charges and van der Waals terms, and these changes are described herein. Several observations concerning the revised parameters may be made here. Our AC–OA, BC–OB, AC–OE and BC–OE bond lengths are shorter than originally chosen [19] to better fit the theoretical B3LYP/6-31G* results. Some force constants have been retained from Homan's [19] revised AMBER force field. One key bending force constant is that associated with the $O–C_{an}–O_{an}$ angle (see Table 1 for atom definitions). In the GLYCAM_93 parameters [22] derived from ab initio calculations, the force constant (K_b) for this bond-angle bend was found to be 110.7 kcal/rad^2. This value can be compared with that used here, 92.6 kcal/rad^2, which is the same as that used by Brady and co-workers [18]. As pointed out previously [22], this is much larger than that used in a previous AMBER modification (40.6 kcal/rad^2) [34], or in a previous GROMOS (68 kcal/rad^2) [35] version. We have used the above K_b value, but different equilibrium φ_0 values, for OE–AC–OA and OE–BC–OB and we believe that this is satisfactory since little stress is put on this angle to achieve the large angle change found between anomers.

Comparison of the empirical energy versus ϕ dihedral angle for the 2-methoxytetrahydropyran gave results in agreement with our B3LYP/6-31G* results and with the ab initio HF/ 6-31G* results shown in Figs. 2 and 3 of Ref. [22]. AMB99C does not have an energy minimum around 160–180° for the axial form, nor was a minimum near 180° found in the ab initio results of Woods et al. [22]. For the equatorial anomer, our minima are in the same positions as found by ab initio calculations [22], but the energy difference between minima is ~ 3.5 kcal/mol rather than ~ 2 kcal/mol found using the HF/6-31G* results. The lowest energy positions for rotation about the ϕ dihedral angle are the same in the two calculations with the lowest-energy conformer being at $\phi = -60°$. The barrier height at $\sim$ 120° is close to the ab initio results in the revised AMB99C being ~ 4.5 kcal/mol. The complete B3LYP/6-31G* geometry optimization results on conformers of 2-methoxytetrahydropyran are presented elsewhere [2].

Fitting of the force constants for bond lengths and angles was carried out using most of the B3LYP/6-31G* minimized structures.

The initial parameter modifications were carried out at the same time gradient-optimized structures were coming from the ab initio studies, and it was found that the bond lengths and angles could be fit to the early structures and did not change significantly when later DFT/ab initio conformers were compared with the empirical structures. The fitting of the empirical conformations to obtain close correspondence to the DFT/ab initio energies and dihedral angles was not particularly straightforward. The complexity of the hydrogen-bond network around the maltose molecule confused the determination of the significant parameters and required that we obtain several more DFT/ab initio conformations than originally planned. For example, it was difficult to distinguish the charge effect (i.e., from atomic charges) from the oxygen van der Waals radii as both contribute to the hydrogen bond energy and geometry. The different combinations of hydrogen bonds from the ten maltose DFT/ab initio conformers allowed resolution of these questions. The hydrogen bonding across the bridging ether group also complicated the determination of the torsional terms around the anomeric carbon and the ether linkage to the reducing residue. It was found that a variety of charge, nonbonded and torsional terms need to be changed, in particular the nonbonded atomic radius (R_i) value of HY was changed from the AMBER value to zero (0.0001). The nonbonded terms of oxygen atoms, OT, OA, OB, and OE were also modified from the original AMBER values to reproduce geometries and energy differences between conformations. The ether ring oxygen, type OE, was found to require a considerably smaller radius than was common in the older AMBER force fields.

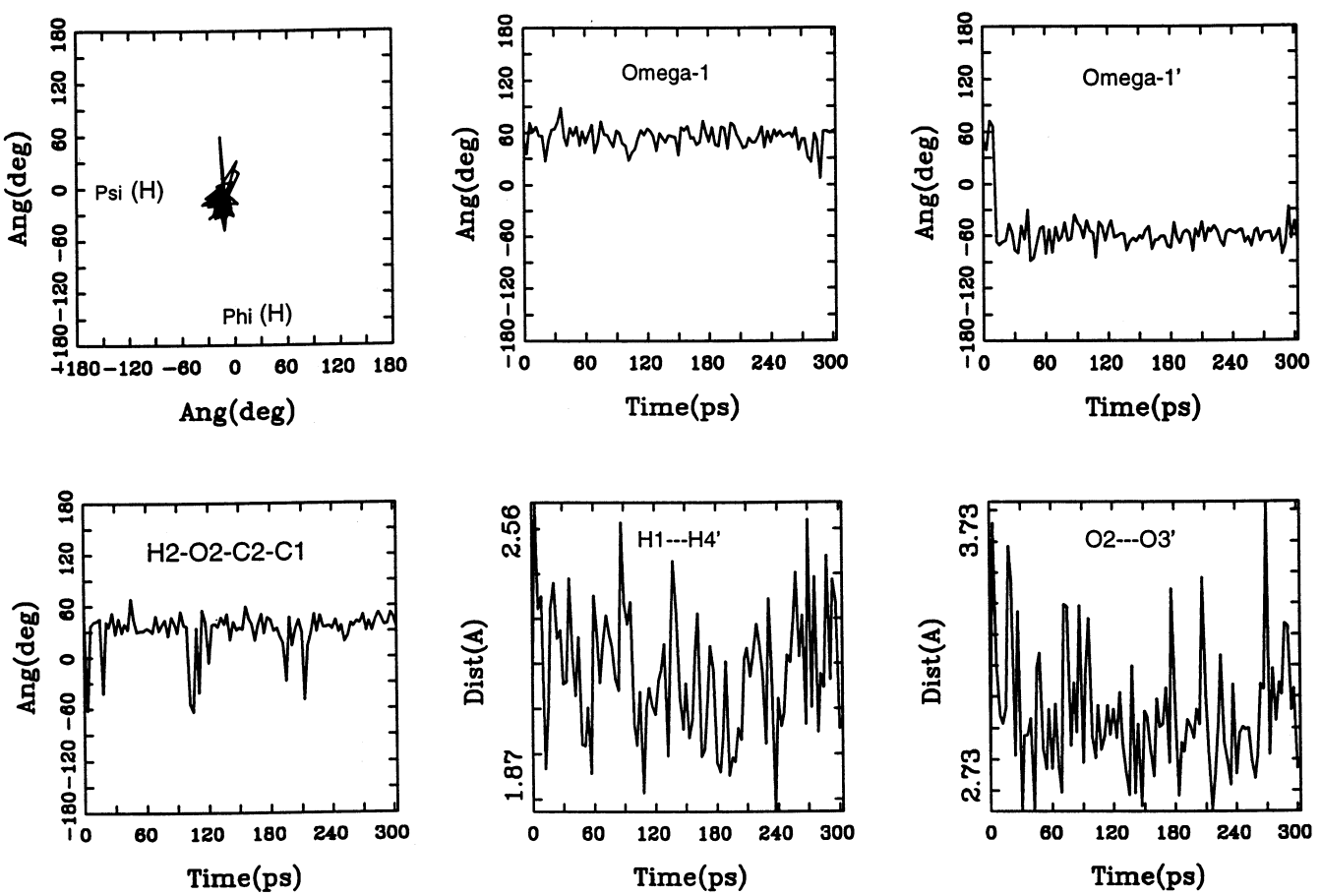

Fig. 3. ϕ_H, ψ_H plot, ω and ψ' plots vs. time, H-1–H-4′ distance vs. time, O-2–O-3′ distance vs. time and the dihedral angle defined by H-2–O-2–C-2–C-1 vs. time from a 300 ps dynamics simulation of α-maltose in vacuo.

Table 1
Structural parameters and energy values for the molecule 2-methoxytetrahydropyran

	Axial form (*gg*) [AMB99C B3LYP/6-31G*]		[MM3 4-21G 6-31G*]			Equatorial form (*tg′*) [AMB99C B3LYP/6-31G*]		[MM3 4-21G 6-31G*]		
	Ref. [2]		Ref. [6]			Ref. [2]		Ref. [6]		
Bond lengths (Å)										
C_{an}–O [a]	1.411	1.422	1.417	1.423	1.388	1.396	1.397	1.406	1.405	1.372
Bond angles (°)										
O_e–C_{an}–O_{an}	113.0	112.7	112.0	111.1	111.9	109.2	108.8	109.6	108.7	109.0
C_{an}–O_{an}–CH_3	114.5	113.1	112.5	115.6	115.2	113.8	113.9	112.5	115.6	115.6
C_{an}–O_e–C4	115.3	113.1			115.5	113.7	111.3			114.0
Dihedral angle (°)										
O5–C_{an}–O_e–CH_3	69.9	61.0	72.6	64.2(61.1) [b]		−58.0	−62.8	−73.6	−63.5(−62.5) [b]	
ΔE (kcal/mol)	0.2	0.0	0.0	0.0	0.0	0.0	1.16	0.5 [c]	3.7	1.5(0.7) [d]

[a] O_e is the ring ether oxygen, C_{an} the anomeric carbon, O_{an} the anomeric oxygen.
[b] Value for MP2/6-31G*.
[c] Results for a dielectric constant of 4.0.
[d] Result for 6-311++G** basis set. The MP2/6-31G* energy of $E=-385.99499$ Hartree can be compared with the DFT(6-31G*) energy of $E=-386.23903$ Hartree for the axial form and $E=-386.23718$ Hartree for the equatorial form.

This result was most obvious from examination of the HO-6···O-5 hydrogen-bond distances found in conformer VIII of the B3LYP/6-31G* geometries [2]. Our revised empirical nonbonded radius for OE still results in HO-6···O-5 distances longer than those from the B3LYP/6-31G* results, but as it turns out, it is in better agreement with the results from a larger basis set [2].

Torsional potentials at the anomeric site were also difficult to fit to all the DFT/ab initio conformations. For example, the global energy minimum has dihedral angles near (0, 0) in (ϕ_H, ψ_H) space. Other somewhat higher energy minima have their backbone dihedral angles near (−52°, −35°) as in Conformer IV of Ref. [2], and at (−44°, −27°) as in Conformer VII of Ref. [2], for example. The latter two conformations are close to the traditional three-fold (±60°, 180°) or sp^3 type torsional terms, but the global energy minimum is at the maximum of energy for such three-fold functional forms. It was not immediately clear just what combination of torsional functions one needed to use to fit both regions of conformational space, and to also fit the 'flipped' conformers where ψ_H values near 180° were obtained. Our approach was to fit as closely as possible the lowest-energy conformations at the expense of the higher-energy structures. For this reason the fit to the dihedral angles of the 'flipped' conformers is not as good as one would like.

We chose not to apply different charges to the anomeric site for the α and β anomers, although the partial atomic charges were changed from previous values. The results of Woods et al. [22] upon fitting electrostatic potentials to various molecules indicated that one might wish to use different partial atomic charges on the C-1 carbon as well as the O-1 and O-5 oxygen atoms for the different anomers being considered. In order to be consistent with previous AMBER parameters, we have not done this. The charges used on the exocyclic hydroxyl groups (OT = −0.650 esu, HY = 0.430 esu and CS = 0.220) are in reasonable agreement with those found previously [11,13,22], while we found that the hydroxymethyl group charges had to differ

slightly (OT = −0.700 esu, HY = 0.430 esu and CT = 0.270) in order to obtain energy differences between conformers that were closer to the DFT/ab initio results and at the same time drive the conformations toward the ab initio results.

The use of the 0.5 scaling factor for both electrostatic and van der Waals 1–4 was examined in detail in the paper by Cornell et al. [1]. However, we can compare a variety of parameters with their results as described. For example, we find the ethane eclipsed–staggered energy difference to be 2.94 kcal/mol relative to 2.89 kcal/mol reported by Cornell et al. [1]. The butane *gt* energy difference is 0.67 kcal/mol versus 0.67 kcal/mol by Cornell et al. [1], while the *cis–trans* energy difference was found to be 5.22 kcal/mol versus 5.16 kcal/mol [1]. All the butane heavy atom angles were within 0.1° of the published AMBER values. For the important case of methanol, we find the *cis–gauche* energy difference of 1.99 kcal/mol to be higher than the original AMBER value of 1.03 kcal/mol, due to the higher barrier to rotation around the CT–OT bond found to be necessary in AMB99C. The hydrogen-bond energy of methanol is also important and depends upon which of the two sets of charges one uses. In the case of the methoxy charge group the ΔE for methanol dimer formation is −6.3 kcal/mol with a 1.889 Å hydrogen bond length. Using the exocyclic hydroxyl charges and atom type, the ΔE value is −5.9 kcal/mol with a 1.904 Å hydrogen bond length. The O–H···O angle of 176.2° and H···O–H angle of 139.3° are in quite reasonable agreement with DFT/ab initio results [2], as are the hydrogen-bond energies and bond lengths [2]. These results can be compared with those obtained from MM3 [36] calculations where ΔE is −5.9 kcal/mol for $\varepsilon = 1.5$, with a very short OH···O hydrogen bond length of 1.75 Å, and an O–H···O angle of 178°.

3. Ab initio, vacuum molecular mechanics, and experimental results

2-Methoxytetrahydropyran.—It has been known for many years that in the axial–equatorial equilibrium of 2-methoxytetrahydropyran the axial form predominates, as is indicated by the measured vicinal coupling constants and dipole moment measurements [37]. Theoretical studies by ab initio methods have been carried out on 2-methoxytetrahydropyran [6,22,38] and 2-hydroxytetrahydropyran [39] and are in agreement with the experimental results. The axial and equatorial linkages were examined, and the geometry around the C–O bond determined by geometry optimization using HF/4-21G and HF/6-31G* basis sets and calculating energies at the MP2/6-31G* level of theory [6]. The authors [6] found that the axial form is favored by 0.84 kcal/mol over the equatorial at the HF/6-31G* level with the *gg* conformation favored. Using DFT methods at HF/6-31G* minima, Tvaroska and Carver [39] also found that 2-hydroxytetrahydropyran preferred the axial form, but after solvation corrections the free-energy difference for axial versus equatorial preference was removed. A comparison of molecular geometry and energies from different calculations is presented in Table 1. Our B3LYP/6-31G* results [2] are in general agreement with previous ab initio studies.

Although the DFT/ab initio calculations give significantly different anomeric bond lengths with different basis sets, it is clear that the bond length of the C_{an}–O_{an} bond shortens upon going from the axial to the equatorial anomer, and that the magnitude of the shortening is about 0.016–0.025 Å. Further, the O_e–C_{an}–O_{an} angle closes upon going from the Axial to the equatorial form by 3–4°, while the C_{an}–O_{an}–CH_3 bond angle is opened relative to the ring ether oxygen by several degrees in the equatorial form, but these angles are nearly the same in the axial form. The trends from our B3LYP/6-31G* calculations are consistent with previous results of DFT/ab initio calculations on 2-hydroxytetrahydropyran [39]. The trend of each of the above parameters is well reproduced using AMB99C, even though the maltose results were the prime structural parameters used in the development of the force field terms. The AMB99C energy difference between anomers is of marginal interest since the two

sets of atom types make this comparison impossible.

Energy component analysis suggests that the AMB99C force field is significantly different from the recent QMFF force field [16], in particular in the magnitude of the torsional (QMFF) terms. The magnitude of the contribution to the total energy from the revised AMB99C torsional term is 0.4 and 0.2 kcal/mol for the axial and equatorial anomers, respectively. This is in contrast to torsional energy values of 28.6 and 31.7 kcal/mol (axial and equatorial anomers, respectively) reported for the QMFF force field. It is not clear why such large torsional terms are found in the QMFF force field since the dihedral angles of the molecules are all near their lowest torsional energy state and should be nearly zero in value.

Other empirical conformational studies of 2-hydroxytetrahydropyran can be found in the paper by Tvaroska and Carver [6], where several empirical studies were reviewed and were shown to be in poor agreement with the ab initio results. In particular, several force fields give the equatorial form to be the energetically preferred one as found here. As expected, the geometry and conformational parameters found using AMB99C are closer to the B3LYP/6-31G* results than those from MM3 calculations, although calculations [40] using MM2CARB described the different energy minima for the axial and equatorial forms with reasonable success.

Glucose.—Recently, computational studies on glucose using ab initio methods [15] have been carried out. Results from these ab initio [15] and other MO studies are compared with the AMB99C results on conformational energy dependencies. In particular, Barrows et al. [15] list (see Tables 1 and 6 in Ref. [15]) the low-energy conformations of glucose as determined by a variety of ab initio methods including some at the MP2 level. The result of these calculations can be summarized as follows. In the gas phase, the axial or α anomer is of lower energy than the equatorial or β anomer, and Conformer 8 (their nomenclature [15] in which the hydrogen-bonding network is counterclockwise and O-5–C-5–C-6–O-6 = *gg*) is generally lowest in energy. The two other rotational forms (*tg* and *gt*) around the C-5–C-6 bond are found to be only slightly higher in energy (0.1–0.5 kcal/mol). Calculations using the AMB99C force field result in the gauche (*gt*) form being lowest in energy with the *tg* = 1.5 kcal/mol and the *gg* = 2.0 kcal/mol higher in energy. Conformer 3 of the β anomer series (C-3–C-4–C-5–O-5 = *t*) was of lowest energy by both ab initio [15] and AMB99C. Several noteworthy geometric parameters include the C-5–O-5–C-1 and O-5–C-1–O-1 bond angles. AMB99C gives 116.0 and 113.1°, respectively, for the trans form (Conformer 7 in Ref. [15]), and these values can be compared with 113.9 and 113.2° from MP2 calculations [15], 115.1 and 108.4° by MM3 [15] and 114.0 and 110.7° from averages of the Cambridge Structural Database (CSD) [41]. The AMB99C distance across the ring from C-1 to C-4 is 2.900 Å, in agreement with the average CSD value of 2.881 Å [41]. The O-1–O-4 distance is slightly longer by AMB99C and by the B3LYP/6-31G* calculations than found from the X-ray diffraction results. This is to be expected, as the center of the oxygen electron cloud on the bridging O-1 atom is moved off the nucleus toward the O-4 direction and results in a shorter X-ray distance than one finds using the nuclear center to define the coordinates. We believe that the B3LYP/6-31G* distance is best used for parameterization. No further analysis of glucose is presented here since the comparison is good throughout the different conformations.

Maltose.—Many studies, both theoretical [2,3,26] and experimental, have been carried out on β-maltose (the β anomer of maltose), and the available neutron diffraction and X-ray structures [42] have been used as guides for parameter development by other authors. DFT/ab initio geometry optimization (B3LYP/6-31G*) was carried out on ten conformations as described [2], and these structures were used in the parameter development described here. Geometry optimization calculations on Conformers I–IV at a more robust (B3LYP/6-311 + + G**) level of theory were also made [2] as tests of the basis set. A discussion of early empirical calculations may

be found in Melberg and Rasmussen [3]. A comparison of calculated and experimental geometry parameters is presented in Table 2. Three of the ten conformations found from the B3LYP/6-31G* geometry optimization are compared with the AMB99C conformations. Experimental data are presented in Table 2 for the neutron diffraction [42] and X-ray structures [43] of maltose and for methyl α-maltotrioside [44]. The lowest-energy DFT/ab initio structure, Conformer I, is structurally very close to the neutron diffraction structure [42] with nearly identical backbone and side-chain dihedral angles. Fig. 1 shows Conformations I, III, and VI of β-maltose with the AMB99C potential atom types, atomic charges and selected dihedral angles, and Conformers II, IV, V, VII, VIII, IX and X are shown as ball and stick models (Fig. 2). The energy differences between conformers for both DFT/ab initio and empirical results are also in Fig. 1. The empirical energy differences between conformations are smaller than those obtained from the B3LYP/6-31G* calculations, although in better agreement with larger basis set results from B3LYP/6311 + + G** calculations [2]. Fig. 3 shows the results of a 300 ps molecular dynamics simulation of β-maltose.

The molecular geometry and energy results presented in Table 2 and Fig. 2 give us information on the flexibility of the maltose molecule with the AMB99C parameters. The variation of dihedral angles in the ϕ_H–ψ_H distribution during the vacuum dynamic simulation is broad, spanning from -35 to $+5°$ in ϕ_H and -43 to $+57°$ in ψ_H. The average ϕ_H–ψ_H values for the 300 ps dynamics run were $(-14, -17°)$. The two ω dihedral angles are predominately in the *gt* conformation, and the exocyclic hydroxyl groups undergo conformation transition jumps between different conformational states. The dihedral angles found for the lowest-energy conformation are close to the mean of three ensemble regions found in recent calculations [18] using a modified CHARMM force field. However, the revised AMB99C potentials do not have a low-energy minimum in the potential energy surface in the region of ϕ_H–ψ_H of $(-61, -40°)$, which differs from several other empirical energy calculations [18]. The closest conformation to this region of ϕ_H–ψ_H space is a B3LYP/6-31G* conformation that upon energy minimization moved to $(\phi_H$–$\psi_H = -53, -35°)$ with a relative energy of 2.27 kcal/mol above the lowest-energy structure. Our results do not closely agree in ϕ_H–ψ_H position with any of the minima found previously by Ha et al. [18], although the results of French and Dowd [46] (ϕ_H, $\psi_H = -16, -24°$) are close to one B3LYP/6-31G* minimum $(-8, -24°)$ with a relative energy of 2.7 kcal/mol. The X-ray [43,44] and neutron diffraction [42] derived structures are of low energy using the newly derived AMB99C force field (see Table 2). Clearly, competition between different hydrogen-bonding patterns in the crystal forms is sufficient to subtly perturb the conformation of the X-ray structure, but the fit between both the DFT/ab initio data and the structures from the empirical potentials to the experimental molecular structures is very encouraging.

The dihedral angles obtained here for the vacuum state are in general agreement with other empirical calculations on β-maltose [3], where ϕ_H, ψ_H values of $(-21, -24°)$, $(17, 19°)$, $(-55, -43°)$, $(-29, -168°)$ and $(-160, -24°)$ were obtained in manifolds of different hydroxyl groups rotations. The authors [3] reviewed the literature of calculations prior to 1979, and these papers will not be referenced further here. Not all of the conformations found by Melberg and Rasmussen [3] are of minimum energy in the revised AMB99C force field; in particular the $(-55, -43°)$ and $(17, 19°)$ regions are not found to be of low energy as stated above. MM3 calculations [47] gave energy minima at ϕ_H and ψ_H of $(-55, -48°)$ for β-maltose, $(-23, -22°)$ for α-maltose, a shallow minimum at $(1, 24°)$ for β-maltose, and $(-31, -168°)$ and $(-28, -170°)$ for β- and α-maltose, respectively. The energy differences between these last minima and the global minima are less than 2 to 3 kcal/mol. More recent calculations on β-maltose using a modified GROMOS potential energy function [26] found the global minimum centered at $(\phi_H, \psi_H) = (-20, -17°)$ in vacuo, moving to $(\phi_H, \psi_H) = (-40, -31°)$ and $(-49, -36°)$ after molecular

Table 2
Geometry and energies of β-maltose from in vacuo calculations, and X-ray and neutron diffraction crystal structures.

	B3LYP/6-31G* Ref. [2]			AMB99C			X-ray Ref. [44]	Neutron Ref. [42]	X-ray Ref. [45]	
	I	III [a]	VI	I	III	VI				
Dihedral angles (°)										
ϕ_H	−9.18	−17.8	−34.2	−4.1	−16.8	−33.5	1	4.8	−38 [b]	−38 [b]
ω_H	5.74	−17.3	−171.4	7.7	−11.3	−141.9	13	13.3	−29	−33
ω	55.7	67.5	71.5	52.5	69.2	35.8		59.1		
ω'	−63.1	−69.2	54.4	−58.2	−67.9	52.7		−62.4		
Ring dihedrals (°)										
C-1–C-2–C-3–C-4	−55.6	−53.0	−50.8	−56.3	−53.2	−53.4	NA	−54.7	−53.7	−52.5
C-2–C-3–C-4–C-5	56.1	55.6	56.9	55.8	57.8	54.5	NA	54.6	54.6	53.6
C-3–C-4–C-5–O-5	−55.8	−59.3	−59.6	−55.1	−59.5	−55.7	NA	−52.4	−56.7	−58.2
C-4–C-5–O-5–C-1	59.1	64.3	61.3	58.6	60.7	60.6	NA	57.2	60.1	62.8
C-5–O-5–C-1–C-2	−58.5	−60.7	−54.4	−59.2	−54.9	−59.9	NA	−58.9	−58.3	−59.0
Angles (°)										
C-5–O-5–C-1	115.4	114.2	116.4	115.3	116.0	115.6	115.8	113.8	114.1	113.8
O-5–C-1–O-1	111.7	111.8	113.3	111.2	111.3	112.9	108.7	109.8	112.8	111.2
C-1–O-1–C-4′	119.2	115.6	119.1	118.0	115.8	121.4	117.2	117.8	114.8	115.4
Nonbonded bond length (Å)										
H(O-2)–O-3′	1.97			1.94				1.81		
H(O-3′)–O-2		1.98			2.00					
H(O-6)–O-3′			2.00			2.10				
O-1–O-4	4.50	4.54	4.68	4.49	4.69	4.54		4.41		
O-1–O-4′	5.48	5.49	5.55	5.49	5.47	5.54		5.47		
Relative energy (kcal/mol)	0.0	2.0	6.4	0.0	1.6	5.6		0.24 [c,d]		

[a] Conformation with all hydroxyl groups in a clockwise orientation.
[b] The geometries of two of the three rings of methyl α-maltotrioside are given [45].
[c] The flexible dihedral angles are nearly the same as conformer I above and close to those of the neutron diffraction study [42].
[d] Results from torsion forcing the ϕ_H and ψ_H dihedral angles to the experimental values listed and subsequent energy minimization using the AMB99C force field with all other geometry treated as flexible.

dynamics simulations using explicit water in boxes of differing sizes. Our results are in reasonable agreement with these results [26] including our solution results which are described in Paper III in this series [28]. However, to our knowledge, no previous empirical energy force field achieved the global energy minimum close to the dihedral angles found from the B3LYP/6-31G* optimization.

Cyclomaltooligosaccharides (cyclodextrins).—To test the resulting potentials further, we have examined several larger α-linked polysaccharides. Cyclodextrins (CDs) are macrocyclic oligosaccharides consisting of from six to several hundred D-glucose units each linked by an α-(1→4) interglucosidic bond. Many CDs can be crystallized from aqueous solutions, although most larger macrocyclics do not easily form crystals that are useful for diffraction studies. We report here studies on α-CD, a ring of six α-linked glucose rings, and β-CD, which has seven α-linked glucose units. We describe the results of calculations on these CDs only as guides to test the new AMB99C parameters. These compounds were not used in the derivation of the parameters, and this is not intended to be a full discussion of these interesting cyclic compounds.

α-CD was constructed using the Polymerizer module in the MSI Polymer Software. The backbone dihedral angles and the dihedral angles of the hydroxyl groups were set as found in the X-ray study of α-CD hydrate [48]. β-CD was built using X-ray and neutron diffraction structures as guides [49–51], and the resulting structures were energy minimized in vacuo. A 100 ps dynamics simulation in vacuo was run on both α-CD and β-CD to allow the molecules to find low-energy states, and the molecules were averaged over the molecular dynamics simulation. The averaged structures were finally energy minimized. The results for our calculations and experimental data for one structure of α-CD are presented in Table 3, while results for a similar simulation on β-CD are presented in Table 4.

It is of interest that the calculated dihedral angles are $\sim 2-3°$ larger than found in the X-ray structure. This variance apparently allows the average O-4(n)–O-4($n-1$)–O-4($n-2$) angle to adjust and is calculated to be nearly identical to that found in the crystal structure. On the other hand, the O-2(n)–O-3($i-1$) distance is calculated to be slightly larger than that found from the crystal structure. The results are most interesting and indicate that even in the vacuum state the AMB99C parameters reproduce the experimental X-ray structure of α-CD very closely. Dynamic simulations on the solvated state will be described in Paper III [28].

The molecule β-CD is of interest because of the possible appearance of 'flipped' residues, i.e., a conformational flip resulting in rotation of the glucose ring by $\sim 180°$. Table 4 presents experimental and calculated molecular parameters for β-CD and allows comparison of the X-ray crystal structure [49,52] with the calculated vacuum states. The calculated ϕ and ψ values are only 5 and 3° from the X-ray crystal structure, respectively, and this is an excellent result considering that no crystal packing or solvent interactions were included in the empirical calculations.

Table 3
Molecular parameters of α-CD from X-ray and empirical AMB99C energy minimization and averages from 100 ps dynamics in vacuo

Parameters	α-CD Experimental [a]	α-CD Calculated Minimum E	α-CD Calculated Dyn Ave. [b]
O-2···O-3($i-1$) (Å)	2.87	2.88	2.91
O-4(i)···O-4($i+1$)–O-4($i+2$) (°)	118.9–119.9	120.0	120.0
O-1···O-4′ (Å)	4.28	4.29	4.28
O-4(i)···C-1(i)–O-4($i+1$)–C-4($i+1$) (°)	170(6)	173(2)	173(2) [c]
C-1(i)–O-4($i+1$)–C-4($i+1$)···O-4($i+2$) (°)	−172(3)	−174(3)	−174(3) [c]

[a] Ref. [47].
[b] The statistical average is over the simulation time course of 10–102 ps.
[c] ϕ_H and ψ_H are ~ -4 and $-9°$, respectively.

Table 4
Crystal and AMB99C energy minimized and dynamics averaged structural parameters of β-CD in vacuo

	Crystal structure Ref. [47]	AMB99C (E min)	AMB99C (Dyn. Ave) [a]
Torsion angles ϕ (°)	av 109.8	115.4 [b]	114.7
O-5(n)–C-1(n)–O-4($n-1$)–C-4($n-1$)	min 102.3		88.5
	max 118.6		137.6
Torsion angles ψ (°)	av 127.6	124.0 [b]	124.6
C-1(n)–O-4($n-1$)–C-4($n-1$)–C-3($n-1$)	min 114.2		90.9
	max 140.4		158.4
Angles (°)	av 128.3	128.5	128.5
O-4(n)–O-4($n-1$)–O-4($n-2$)	min 125.2		125.4
	max 132.5		130.4
Distances (Å)	av 4.385	4.41	4.40
O-4(n)–O-4($n-1$)	min 4.267		3.93
	max 4.499		5.03
Distances (Å)	av 2.884	2.89	2.80
O-2(n)–O-3($n-1$)	min 2.801		2.63
	max 2.978		3.63

[a] Statistical average is over 100 ps dynamics at 300 K, not including the period 60–72 ps during which time the conformation of one residue flipped to the region, $\phi \sim 50°$, $\psi \sim -135°$.
[b] The equivalent ϕ_H and ψ_H values are approximately; -5 and $+6°$, respectively.

Interestingly, the O-4(n)–O-4($n-1$)–O-4($n-2$) angle remained at the experimentally determined value even though the dynamically averaged dihedral angles are 5° larger in ϕ and 3° smaller in ψ. The cross-ring distances, O-4(n)–O-4($n-1$), are fairly constant with a larger variance than found experimentally, as would be expected for the vacuum case. Similarly, the O-2(n)–O-3($n-1$) distance is much more flexible in the vacuum case than found experimentally.

Unlike previous calculations on β-CD, [53,54] where the GROMOS force field was used with TIP3P waters in a box with dimensions of $22.1 \times 23.1 \times 25.1$ Å, we do not see a large distribution of ϕ and ψ dihedral angles. Rather, we observe dihedral angles remaining close to the experimentally determined structure with no bimodal distribution. The exception to this is during the time period that one residue 'flipped' into another conformation. The 'flipped' conformation resulted in a distortion in the seven-membered ring shape, but it was transitory (12 ps) and reverted to the standard molecular dimensions afterward. The solvation studies are presented in Paper III [28], where we show that the 'flipped' conformation is much more stable in water than in vacuo. Lipkowitz [55] found that somewhat long and narrow structures were preferred in vacuo. We do not find a wide range of structural differences as the simulation proceeds, although the molecule is very flexible during dynamics and could take up different shapes with only little external energy included from inclusion complexes or crystal packing forces. A review of published studies using molecular mechanics and dynamics simulations on β-CD can be found in the review by Lipkowitz [56].

4. Conclusions

Results presented here show that the B3LYP/6-31G* structural parameters can be approximated by a revised AMBER empirical force field, AMB99C, and that these potentials will be useful in further carbohydrate studies. Conformation I, found from DFT/ab initio calculations, was not easy to reproduce by previous empirical force fields, and AMBER required modifications to achieve a reasonable fit for the ten DFT/ab initio structures. We have not achieved a totally satisfactory fit for

every DFT/ab initio conformation as seen in Fig. 1. However, the tests of the potentials described herein, as well as other tests of our AMB99C force field [57], show clearly that fitting high level DFT/ab initio molecular geometries and energies can result in empirical structures with high correlation to experimental geometry and conformation.

Uncited reference

[45]

Appendix A

Revised force field: AMB99C

Atom types

CS	Carbohydrate sp^3 ring carbon
AC	Alpha-anomeric sp^3 carbon
BC	Beta-anomeric sp^3 carbon
AH	Alpha-anomeric hydrogen on AC
BH	Beta-anomeric hydrogen on BC
OA	Alpha-anomeric oxygen
OB	Beta-anomeric oxygen
OE	Carbohydrate ring oxygen (ether)
OT	Carbohydrate hydroxyl oxygen
HY	Carbohydrate hydroxyl polar hydrogen
HT	Carbohydrate hydrogen on sp^3 carbon

Quadratic bond

i	j	R_o	k
AC	OA	1.403	334.3
BC	OB	1.390	334.3
CS	OA	1.420	334.3
CS	OB	1.430	334.3
CS	OE	1.425	296.7
AC	OE	1.400	296.7
BC	OE	1.414	296.7
CT	OT	1.414	334.3
CS	CS	1.514	214.8
CS	CT	1.514	214.8
CS	OT	1.416	334.3
AC	CS	1.519	214.8
BC	CS	1.523	214.8
BC	BH	1.099	337.3
AC	AH	1.099	337.3
OT	HY	0.966	460.5

Quadratic angles

i	j	k	θ	$k-\theta$
AC	OA	HY	107.8	53.6
BC	OB	HY	109.35	53.6
AC	OA	CS	115.3	75.0
AC	OA	CT	113.0	62.0
BC	OB	CS	115.0	62.0
BC	OB	CT	112.0	62.0
CS	OE	AC	111.9	90.7
CS	OE	BC	111.9	90.7
CS	AC	OA	105.0	81.0
CS	BC	OB	106.0	81.0
AH	AC	OE	106.7	45.2
AH	AC	OA	109.4	45.0
BH	BC	OE	107.85	45.2
BH	BC	OB	109.89	45.9
AC	CS	OT	109.5	45.0
BC	CS	OT	111.0	75.0
CS	CS	CT	110.3	38.0
CS	CS	AC	111.7	38.0
CS	CS	BC	110.7	45.0
CS	CS	OA	107.8	45.0
CS	CS	OB	109.5	45.2
CS	CT	OT	113.1	45.0
CS	CS	OT	109.9	45.0
CS	CS	OE	108.9	81.0
CT	CS	OE	107.0	45.0
CS	AC	OE	109.7	81.0
CS	BC	OE	108.8	81.0
CS	OE	CS	111.0	90.7
OE	AC	OA	111.55	92.6
OE	BC	OB	108.5	92.6
CT	OT	HY	107.0	35.0
CS	OT	HY	109.75	53.6
HT	CS	OT	110.2	45.0

Missing values are assumed to be 0.0.

Torsion 3-fold

i	j	k	l	k_1	θ_1	k_2	θ_2	k_3	θ_3
·	CS	CS	*						0.40
CS	CS	CS	CT						0.20
CS	CS	CS	AC						0.34
*	CS	CT	*						1.20
OE	CS	CT	OT						1.20

Torsion 3-fold

i	*j*	*k*	*l*	k_1	θ_1	k_2	θ_2	k_3	θ_3
·	AC	CS	*						1.00
·	BC	CS	*						1.02
·	CS	OT	*						0.75
·	CS	OE	*						0.50
·	BC	OT	*						0.20
·	BC	OB	*						0.483
·	BC	OE	*						0.50
·	AC	OA	*						0.00
AH	AC	OA	CS	0.4	180.0	1.00	180.0		1.80
CS	AC	OA	CS			1.70	180.0		0.50
·	AC	OE	*						0.50
AC	CS	OT	HY	1.5	180.0				1.30
BC	CS	OT	HY						1.02
CS	CS	OT	HY						1.12
CS	CT	OT	HY						1.02
·	CT	OT	*						1.00
HT	CS	OA	AC			1.50			1.00
·	CS	OA	*						2.30
OE	AC	OA	CT	−0.5		0.5	180.0		0.928
CS	AC	OA	HY						0.85
OE	AC	OA	HY	0.0	0.0				
OE	BC	OB	CT	0.5	180.0				0.928
BH	BC	OB	CS			2.25	240.0		
CS	BC	OB	CS	0.0					0.0
OE	BC	OB	HY	0.0					0.70
BH	BC	OB	HY	0.0					
CS	BC	OB	HY	0.0					1.0

Missing values are assumed to be 0.0.

Nonbonded 6–12 terms

i	R_i	eps−*I*
HY	0.0001	0.0001
HT	3.200	0.0045
AH	2.936	0.0045
BH	2.936	0.0045
CS	3.816	0.1094
OT	3.630	0.165
OA	3.470	0.165
OB	3.850	0.165
OE	2.400	0.450

Bond increment

AC	OE	0.000	−0.000
BC	OE	0.000	−0.000
AC	OA	0.200	−0.200
BC	OB	0.200	−0.200
CS	OA	0.000	0.000
CS	OB	0.000	0.000
CS	OT	0.220	−0.220
CS	OE	0.200	−0.200
CS	HT	0.000	0.000
CS	CT	0.000	0.000
CS	AC	0.000	0.000
CS	BC	0.000	0.000
OT	CT	−0.270	0.270
OT	HY	−0.430	0.430
OA	HY	−0.430	0.430
OB	HY	−0.430	0.430
CT	HC	0.000	0.000
AC	HA	0.000	0.000
BC	BH	0.000	0.000

References

[1] W.D. Cornell, P. Cieplak, C.I. Bayly, I.R. Gould, K. Merz, D.M. Ferguson, D.C. Spellmeyer, T. Fox, J.W. Caldwell, P.A. Kollman, *J. Am. Chem. Soc.*, 117 (1995) 5179–5197.

[2] F.A. Momany, J.L. Willett, *J. Comp. Chem.*, submitted for publication.

[3] S. Melberg, K. Rasmussen, *Carbohydr. Res.*, 76 (1979) 23–37.

[4] S. Melberg, K. Rasmussen, *Carbohydr. Res.*, 69 (1979) 27–38.

[5] S. Melberg, K. Rasmussen, *Carbohydr. Res.*, 71 (1979) 25–34.

[6] I. Tvaroska, J.P. Carver, *J. Phys. Chem.*, 98 (1994) 9477–9485.

[7] M. Dauchez, P. Derreumaux, P. Lagant, G. Vegoten, *J. Comput. Chem.*, 16 (1995) 188–189.

[8] C.J.M. Huige, C. Altona, *J. Comput. Chem.*, 16 (1995) 56–79.

[9] M. Odelius, A. Laadsonen, G. Widmalm, *J. Phys. Chem.*, 99 (1995) 12686–12692.

[10] B.J. Hardy, A. Gutierrez, K. Lesiak, E. Seidl, G. Widmalm, *J. Phys. Chem.*, 100 (1996) 9187–9192.

[11] H. Senderowitz, C. Parish, C. Still, *J. Am. Chem. Soc.*, 118 (1996) 2078–2086.

[12] H. Senderowitz, W.C. Still, *J. Org. Chem.*, 62 (1997) 1427–1438.

[13] W. Damm, A. Frontera, J. Tirado-Rives, W.L. Jorgensen, *J. Comput. Chem.*, 18 (1997) 1955–1970.

[14] D.R. Ferro, P. Fumilia, M. Ragazzi, *J. Comput. Chem.*, 18 (1997) 351–367.

[15] S.E. Barrows, J.W. Storer, C.J. Cramer, A.D. French, D.G. Truhlar, *J. Comput. Chem.*, 19 (1998) 1111–1129.

[16] M.-J. Hwang, M. Waldman, C.S. Ewig, A.T. Hagler, *Biopolymers*, 45 (1998) 435–468.

[17] L. Norskov-Lauritsen, N.L. Allinger, *J. Comput. Chem.*, 5 (1984) 326–335.

[18] S.N. Ha, L.J. Madsen, J.W. Brady, *Biopolymers*, 27 (1988) 1927–1952.

[19] S.W. Homans, *Biochemistry*, 29 (1990) 9110–9118.

[20] C.J. Edge, U.C. Singh, R. Bazzo, G.L. Taylor, R.A. Dwek, T.W. Rademacher, *Biochemistry*, 29 (1990) 1971–1974.

[21] P.D.J. Grootenhuis, C.A.G. Haasnoot, *Mol. Simul.*, 10 (1993) 75–95.

[22] R.J. Woods, R.A. Dwek, C.J. Edge, B. Fraser-Reid, *J. Phys. Chem.*, 99 (1995) 3832–3846.
[23] T.M. Glennon, T.J. Zheng, S.M. LeGrand, B.A. Shutzberg, K.M. Merz Jr., *J. Comput. Chem.*, 15 (1994) 1019–1040.
[24] J. Koca, S. Perez, A. Imberty, *J. Comput. Chem.*, 16 (1995) 296–310.
[25] M.L.C.E. Kouwijzer, P.D.J. Grootenhuis, *J. Phys. Chem.*, 99 (1995) 13426–13436.
[26] K. Ott, B. Meyer, *J. Comput. Chem.*, 17 (1996) 1068–1084.
[27] J. Fabricius, S.B. Engelsen, K. Rasmussen, *J. Carbohydr. Chem.*, 16 (1997) 751–772.
[28] F.A. Momany, J.L. Willett, *Carbohydr. Res.*, 326 (2000) 210–226.
[29] IUPAC-IUB Commission on Biochemical Nomenclature (a) *J. Mol. Biol.*, 52 (1970) 1–17. (b) *Arch. Biochem. Biophys.*, 145 (1971) 405–421. (c) *Eur. J. Biochem.*, 18 (1971) 151–170, and Nomenclature of Carbohydrates, document 24.10, Royal Society of Chemistry, Cambridge.
[30] S. Perez, M. Kouwijzer, K. Mazeau, S.B. Engelsen, *J. Mol. Graphics*, 14 (1996) 307–321.
[31] F.A. Momany, V.J. Klimkowski, L. Schäfer, *J. Comput. Chem.*, 11 (1990) 654–662.
[32] F.A. Momany, R. Rone, *J. Comput. Chem.*, 13 (1992) 888–900.
[33] L. Schafer, S.Q. Newton, F.A. Momany, V.J. Klimkowski, *J. Mol. Struct.*, 232 (1991) 275–289.
[34] J.N. Scarsdale, P. Ram, J.H. Prestegard, R.K. Yu, *ACS Symp. Ser.*, 430 (1989) 246–265.
[35] J.E.H. Koehler, W. Saenger, W.F. van Gunsteren, *Eur. Biophys. J.*, 15 (1987) 197–210.
[36] A.D. French, D.P. Miller, *ACS Symp. Ser.*, 569 (1994) 235–251.
[37] A.J. de Hoog, E. Havinga, *Recl. Trav Chim. Pays-Bas*, 89 (1970) 972–979.
[38] K.B. Wiberg, M.A. Murcko, *J. Am. Chem. Soc.*, 111 (1989) 4821–4828.
[39] I. Tvaroska, J.P. Carver, *Carbohydr. Res.*, 309 (1998) 1–9.
[40] I. Tvaroska, S. Perez, *Carbohydr. Res.*, 149 (1986) 389–410.
[41] A.D. French, R.S. Rowland, N.L. Allinger, *ACS Symp. Ser.*, 430 (1989) 120–140.
[42] M.E. Gress, G.A. Jeffrey, *Acta Crystallogr., Sect. B*, 33 (1977) 2490–2495.
[43] G.A. Jeffrey, R.K. McMullan, S. Takagi, *Acta Crystallogr., Sect. B*, 33 (1977) 728–737.
[44] G.J. Quigley, A. Sarko, R.H. Marchessault, *J. Am. Chem. Soc.*, 92 (1970) 5834–5839.
[45] W. Pangborn, D. Langs, S. Perez, *Int. J. Biol. Macromol.*, 7 (1985) 363–369.
[46] A.D. French, M.K. Dowd, *J. Mol. Struct.* (*Theochem.*), 286 (1993) 183–201.
[47] M.K. Dowd, J. Zeng, A.D. French, P.J. Reilly, *Carbohydr. Res.*, 230 (1992) 223–244.
[48] R. Puliti, C.A. Mattia, L. Paduano, *Carbohydr. Res.*, 310 (1998) 1–8.
[49] K. Linder, W. Saenger, *Carbohydr. Res.*, 99 (1982) 103–115.
[50] C Betzel, W. Saenger, B.E. Hingerty, G.M. Brown, *J. Am. Chem. Soc.*, 106 (1984) 7545–7557.
[51] V. Zabel, W. Saenger, S.A. Mason, *J. Am. Chem. Soc.*, 108 (1986) 3664–3673.
[52] W. Saenger, J. Jacob, K. Gessler, T. Steiner, D. Hoffman, H. Sanbe, K. Koizumi, S.M. Smith, T. Takaha, *Chem. Rev.*, 98 (1998) 1787–1802.
[53] A.M.C. Myles, D.J. Barlow, G. France, M.J. Lawrence, *Biochem. Biophys. Acta*, 1199 (1994) 27–36.
[54] M. Prabhakaran, *Biochem. Biophys. Res. Commun.*, 178 (1991) 192–197.
[55] K.B. Lipkowitz, *J. Org. Chem.*, 56 (1991) 6357–6367.
[56] K.B. Lipkowitz, *Chem. Rev.*, 98 (1998) 1829–1873.
[57] F.A. Momany, J.L. Willett, ANTEC '99, Plastics-Bridging the Millennia, *Proc. SPE 57th Ann. Tech. Conf.*, 1999, pp. 2402–2406.